

## **QUANTUM CHEMISTRY APPLICATIONS IN PREDICTING MOLECULAR**

### **PROPERTIES**

**JAGVIR SINGH**

Department of Chemistry, Nirwan University Jaipur, Rajasthan

**DOI:ijmra.ijesm.66387.88733**

### **ABSTRACT**

*The ability to predict molecular properties thanks to quantum chemistry has revolutionized our understanding of and ability to manipulate matter at the nuclear and molecule scales. A basic problem in quantum chemistry is the prediction of molecular properties, which has the potential to speed up many areas of investigation, such as substance discovery and medication design. Conventional analyses in the context of material science's Density Functional Theory (DFT) prove to be laborious when it comes to atom-by-atom prediction. Recently, AI methods that consider large amounts of rule-based data have also demonstrated potential solutions for this problem. Whatever the case, current arrangements generally underexplores the intricate innate quantum cooperation's of atoms. We present a flexible and generalizable in this study. To predict chemical characteristics, a multilayer graph convolutional neural network (MGCN) is used. More specifically, we preserve the intrinsic structure of each particle by treating it as a graph. Furthermore, the overall planned multiple tiered graph neural network follows the multilevel connections and extracts highlights from the spatial and compliance data with ease. As a result, the multilevel generally speaking depiction can be used to make the forecast. Comprehensive tests on balancing and off-harmony atom datasets show the appropriateness of our concept. Moreover, the comprehensive findings demonstrate the flexibility and generalizability of MGCN for the predicted.*

**Keywords:** *Quantum Chemistry, Predicting Molecular Properties, Density Functional Theory, Multilevel Graph Convolutional Neural Network*

### **1. INTRODUCTION**

The fascinating and incredibly specialized discipline of quantum chemistry, which lies inside the broader field of chemistry, has completely changed our understanding of molecular characteristics and how they behave at the quantum level. The application of quantum physics to explain the erratic dance of electrons inside particles and particles is at

the heart of this field. When it comes to unraveling the perplexing behavior of problems at the smallest scales, quantum chemistry comes in handy, providing tidbits of information on the fundamentals of material reactivity, structure, and characteristics. Its expectation of molecular characteristics is one of its most important commitments; this task is essential to the advancement of several logical domains, from materials science to sedate plan.

In this study, we will delve into the complex world of applications for quantum chemistry, specifically focusing on its critical role in molecular property prediction. Quantum chemistry allows us to comprehend the behavior of electrons and cores by bending the rules of quantum physics, which paves the way for the computation of many molecule properties. This comprehensive analysis provides scientists with an extensive toolkit, enabling them to make informed decisions on innovative particles, materials, and pharmaceuticals in the plan.

Before embarking on this journey, we shall first untangle the fundamental principles of quantum chemistry, including its remarkable approach to understanding the subatomic universe. After that, we shall delve into the plethora of exactly predictable molecular properties, including energies, reactivity, electronic spectra, and molecular designs, to name just a few. We will also explore the practical implications of these expectations in several rational and contemporary applications, illustrating how quantum chemistry has transformed the way we advance and develop in diverse domains such as chemistry, physical science, and science.

We hope to shed light on the important role that quantum chemistry plays in forecasting molecular properties through our examination of this aspect of the subject. It promises to continue influencing the course of science and innovation in an infinite number of ways. It is an example of the amazing power of the human mind and inventiveness in unlocking the mysteries of the little world.

## **2. LITERATURE REVIEW**

Deals, P. J. and Johnson, B. R. (2018). This overview study serves as a fundamental reference by providing a broad perspective on the tactics and approaches utilized in quantum chemistry to predict molecular properties. A thorough description of the theoretical and computational tools, together with their possible applications in various material frameworks, is provided by Johnson and Deals. They look at the evolution of these quantum chemical processes over time and explore their actual potential for various uses. Deep dive into the fundamental role of quantum chemistry in drug disclosure by

Korth, M., and Mayes, H. B. (2020). The importance of accurately forecasting molecular characteristics for the purpose of designing and improving therapeutic molecules is emphasized in the study. It describes how quantum chemistry plays a key role in comprehending the molecular relationships that underpin pharmacokinetics, bioavailability, and drug-receptor blocking, ultimately advancing the development of more safe and effective pharmaceuticals.

In their 2009 survey, Cramer, C. J., and Truhlar, D. G. explore how solvation models and quantum chemistry might be combined to predict molecular features. They discuss the challenges of physically simulating atoms in arrangement and demonstrate how quantum chemistry combined with state-of-the-art solvation models may accurately predict features such as solvation energies and designs. This strategy has broad applications in chemistry, encompassing material science, natural chemistry, and catalysis.

The comprehensive study by Shao, Y., and Head-Gordon, M. (2015) discusses how quantum chemistry can be used to predict spectroscopic features in intricate molecular structures. The paper covers a wide range of techniques, including vibrational spectroscopy, UV-Vis, NMR, and EPR, and highlights the development of computational algorithms and their applications in comprehending complex molecular spectra. It highlights the role that quantum chemistry plays in elucidating the intricate behaviours of molecules and provides tidbits of information on the fundamental theoretical frameworks that enable these predictions to be plausible.

Furche, F. and D. Rappoport (2010). The goal of the work is to create property-enhanced Gaussian premise sets for molecular reaction estimations, with a focus on computational chemistry. The authors investigate the role of fitting premise sets in accurately illustrating the polarizabilities and hyperpolarizabilities of chemical reactions. They explore the efficient upgrading of these premise sets to work on the exactness of quantum synthetic expectancies for a multitude of molecular attributes, ultimately enhancing our understanding of how we might interpret intricate molecule structures and their spectroscopic behaviour.

### **3. MULTILEVEL GRAPH CONVOLUTIONAL NETWORK**

In this part, we first formally present the issue of molecular property assumption. From that point forward, we present our Multilevel Graph Convolutional Network exhaustively.

#### **3.1. Problem Statement**

It is standard methodology to regard particles as complete graphs, with vertices addressing atoms and edges addressing compound bonds. In this sense, a bunch of particles with  $|V| = N$  is alluded to as  $G(V, E)$ , and  $V$  with regards to molecular plan. Assuming that every molecule is in communication with every other molecule, we view the graph as completely undirected, and the edge arrangement satisfies the equation  $|E| = N(N - 1)/2$ . Each  $E$  in this instance comprises two different types of data: edge type and geographic data. Our goal is to create a regressor that can predict particle attributes. Formally speaking, we may describe the problem as:

$$g(f(G)) = y, \quad (1)$$

If  $y$  is the desired attribute to predict and molecular representations are learned using the centre capability  $f: G \rightarrow \mathbb{R}^{N \times D}$ . At that time,  $g$  fully transfers the obtained highlights to the final result. There is generally multilayer cooperation in graph architectures. Within particle physics, actual experts design various balancing functions to represent the nuclear environment by considering correlations at different energies. Motivated by this idea, we attempt to demystify the complexity of molecular cooperation's by modelling quantum cooperation's in particles by addressing the communications between two, three, and more iotas at a level by level.

### 3.2. Network Architecture

**Overview.** In a high-level discussion, the entire engineering might be separated into three categories aside from these data sources. The underlying data is a graph made up of an atom's Euclidean distance framework and a list of all the particles. The Outspread Premise Capability (RBF) layer and the inserting layer are included in the pre-handling portion. While the Spiral Premise Capability (RBF) layer entirely transforms the distance network into a distance tensor, the implanting layer creates molecule and edge embeddings. A few collaboration layers that aim to learn diverse hub depictions at different levels are included in the following MGCN essay. The readout layer, which produces the final result, is the final step.

**Embedding Layer.** A particle's fundamental building blocks are its bonds and atoms. In order to demonstrate partnerships with the least amount of data loss possible, we thus introduce an implanting layer that allows graph vertices and edges to be easily inserted into vectors. The main picture, which we will call the particle embedding here, is no different for atoms having about similar measure of protons in their atomic centers. Using the chemical compound  $\text{CH}_2\text{O}_2$ , Figure 2's information section enumerates five different types

of atoms and their accompanying tone designations. By using the widely used implanting technique, we construct a  $5 \times D$  network with lines linking atoms of the same kind having values that are comparable. Iota embeddings for each compound component are produced at random prior to processing. Similar to molecular embeddings, pair-wise embeddings  $e \in \mathbb{R}^D$  are initiated (Figure 1). For the edges corresponding to comparable atom configurations, this gives us  $E \in \mathbb{R}^{N \times N \times D}$  and equivalent initial edge implanting. In particular,  $e_{ij}$  shows the edge installing of the link between the  $j$ -th particle and the  $i$ -th molecule. Only the inherent property of broken bonds and atoms is related to the pictures generated by the implanting layer. The partnership's terms are displayed in a later subnetwork.

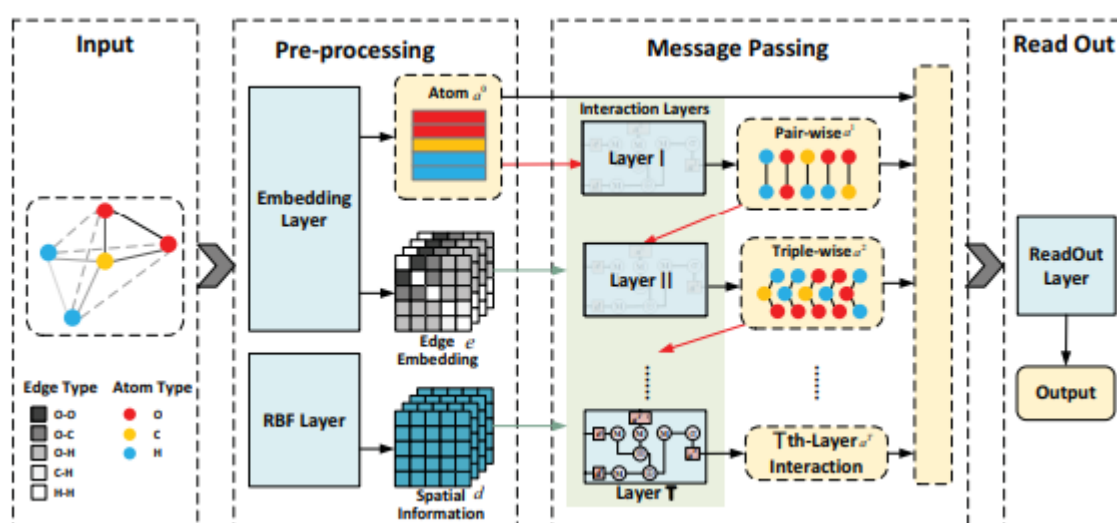


**Figure 1:**The MGCN's overall architecture

**Radial Basis Function Layer.** The degree of cooperation among hubs is influenced by the spatial data, which we convert entirely to strong distance tensors for further use using the RBF Layer. To remove the unpleasant effect of direction, outline determination, we first modify the primitive directions of the atoms to a distinct grid. Furthermore, a distance tensor is entirely constructed from the distance lattice using Spiral Premise Capabilities. The wide and far bit technique known as RBF was initially created to add capability. Its diversity was useful in producing a distinguishing mark, like a particle descriptor. Given an assortment of  $K$  basic worries  $\{\mu_1, \dots, \mu_K\}$ , the single data point  $x$ , explicitly one sets wise distance in the molecule, will be considered as follows:

$$RBF(x) = \prod_{i=1}^k h(\|x - \mu_i\|). \quad (2)$$

For this situation, the documentation  $\sim$  recommends a connection, and the standard is Euclidean distance. In light of the idea in (Schutt et al. 2017a ``), we utilize Gaussian

$\exp(-\beta\|x - \mu\|_2)$  for the extended reason ability  $h$  to stay away from the long level on the fundamental times of the readiness technique.

**Interaction Layer.** we plan our participation layer by the dynamic plan level by level. In the  $l$ -th association layer, we explicitly describe the particle depiction  $a^{l+1}$  and edge depiction  $e^{l+1}$  as:

$$e_{ij}^{l+1} = h_e(a_i^l, a_j^l, e_{ij}^l), \quad (3)$$

$$a_i^{l+1} = \sum_{j=1, j \neq i}^N h_v(a_i^l, e_{ij}^l, d_{ij}), \quad (4)$$

where  $h_v$  is the capacity to accumulate information from the neighbors of the  $l$ -th particle to make a  $l+1$  I, and  $h_e$  is used to refresh edge portrayal.

This staggered exhibition permitted MGCN to show its quantum coordinated effort and effectively safeguard every iota's design. To be more exact, a 0 I inside the main layer shows the molecule embedding that represents the natural properties of explicit compound constituents. A 1 I is comprised of the geographic data and first-demand neighborcenter, and the message is passed by means of a 0,  $e$ , and  $d$  as the forward construing stages. Along these lines, a 2 I tends to significantly increase wise connections, a 3 I represents participation between four centers, etc. Following each cooperation layer, we obtain atom representations reflecting higher-request communications due to particle disintegration, as illustrated in Figure 2.

He is identified as having the update capability:

$$h_e = \eta e_{ij}^l \oplus (1 - \eta) W^{ue} a_i^l \odot a_j^l. \quad (5)$$

where  $\eta$  is the hyper-boundary (default esteem = 0.8) that regulates the influence of prior pairwise data. Here, the symbols  $\odot$  and  $\oplus$  denote the component-wise location as well as individually. In this sense, the associated nuclear representations of the preceding cooperation layer modify the edge implanting.

The potential In order to represent the particle at a higher level of request,  $h_v$  employs message forwarding. Thus, it officially interfaces the center, edge, and space information:

$$h_v = \sigma(W^{uv}(M^{fa}(a_j^l) \odot M^{fd}(d_{ij}) \oplus M^{fe}(e_{ij}))), \quad (6)$$

**Readout Layer.** The connection layers are followed by several levels of particle depictions. In the last phase, we use these highlights to construct a readout layer that emphasizes the ultimate expectation even more.

Above all, as can be seen below, we combine the several particle representations to get the final vertex highlight map:

$$\mathbf{a}_i = \frac{T}{k-0} \mathbf{a}_i^k, \quad (7)$$

where  $\text{—}$  denotes a link and T shows the number of communication layers.

Additionally, we want to foresee the molecule property utilizing multilevel portrayals of every particle. we can show conceivable energy surfaces as follows:

$$E = \sum_i^N \sum_j^N E_{ij}, \quad (8)$$

where E represents outright energy and Eij for the energy connected with the connection between the I-th and j-th atoms ( $I \neq j$ ). In addition, the fragmentary energy ascribed to the I-th particle could be viewed as Eii. As needs be, we can address every depiction autonomously prior to arranging them:

$$\hat{\mathbf{y}} \sum_{i=1}^N W^{r_1^a} \sigma(M^{r_1^a}(\mathbf{a}_i)) + \sum_{i=1}^N \sum_{j=1}^N W^{r_2^a} \sigma(M^{r_2^a}(\mathbf{e}_{ij})), \quad (9)$$

where  $\sigma$  represents the ability to initiate, and more specifically, the delicate as well as work. The commitment of quantum links that intended to every iota is implied by the prior word. Additionally, the final option period represents the edge-related commitment that is not able to be scheduled for a single molecule. The final option term is more complex since particle-related cooperation's make up a greater portion of molecular partnerships. Therefore, we are likely to miss the final option phrase when there is less information.

To set up this model, we utilize the Root-Mean-Square Mistake (RMSE) as our misfortune capacity:

$$\ell(\hat{\mathbf{y}}, \mathbf{y}) = \sqrt{|\hat{\mathbf{y}} - \mathbf{y}|^2}, \quad (10)$$

where  $\mathbf{y}$  is the genuine worth and  $\hat{\mathbf{y}}$  is the expected worth.

## 4. EXPERIMENTS

We carry out tests to show MGCN's applicability from several perspectives: 1) Visionary execution; 2) Multilevel construction viability; 3) Acceptance of generalizability; 4) Verification of adaptability; 5) Variable Number of Connection Layers' Effect.

### 4.1. Datasets

**QM9.** Among benchmark datasets, QM91 is probably the most well-known, containing 134k harmony atoms with their 13 distinct properties. DFT calculates the general casual computations and the properties of all 134k particles. The DFT fallacy is the observational



error evaluation of DFT based techniques. Additionally, the QM9 dataset offers synthetic precision, which the chemistry world generally views as a relatively ideal exactness.

**ANI-1.** The full energies of 20 million off-balance particles are accessible in the ANI-12 dataset, which is many times larger than QM9.

## 4.2. Experimental Setup

Our MGCN is prepared by combining the scaled down group stochastic slope plummet (smaller than usual cluster SGD) with the Adam enhancer. We pick 90% of the cases for readiness, 5% for endorsement, and 5% for testing aimlessly from the bigger ANI-1. Our assessment measurement of decision is Mean By and large Mistake (MAE), which makes it simple to contrast results with baselines.

### 4.2.1. Baselines

We contrast our model with the seven traditional approaches, which might be divided into two categories.

The primary set comprises of three regular AI models with physically produced features extricated from the molecular text. These AI models incorporate Inconsistent Woods (RF) and Piece Edge Backslide (KRR).

## 4.3. Experimental Results

**Predictive performance.** We utilize two datasets to contrast our model and the recently referenced benchmark models. Table 1 gives the engineered accuracy, DFT screw up, and MAE of baselines and our strategy for every one of the 13 properties. The ANI-1 show assessment is shown in Table 2.

**Table 1:** Accuracy of prediction across several models in QM9

| Propertie<br>s | U0  | U   | G   | H   | Cv       | $\epsilon$ HOMO | $\epsilon$ LUMO | $\Delta\epsilon$ | $\omega$ 1       | Z<br>P<br>V<br>E | $\langle R$<br>2)<br>2) | $\mu$                 | $\alpha$              |
|----------------|-----|-----|-----|-----|----------|-----------------|-----------------|------------------|------------------|------------------|-------------------------|-----------------------|-----------------------|
| Unit           | eV  | eV  | eV  | eV  | cal/molK | eV              | eV              | eV               | cm <sup>-1</sup> | e<br>V           | B<br>oh<br>r2           | D<br>e<br>b<br>y<br>e | B<br>o<br>h<br>r<br>3 |
| DFT<br>Error   | 0.2 | 0.2 | 0.2 | 0.2 | 0.35     | -               | -               | -                | 30               | 0.<br>00<br>99   | -                       | 0<br>.<br>2           | 0<br>.<br>5           |



|                  |             |             |               |               |              |               |               |               |             |                     |               |                            |                       |
|------------------|-------------|-------------|---------------|---------------|--------------|---------------|---------------|---------------|-------------|---------------------|---------------|----------------------------|-----------------------|
| Chemical<br>Acc. | 0.04<br>5   | 0.04<br>5   | 0.045         | 0.045         | 0.06         | 0.045         | 0.045         | 0.045         | 12          | 0.<br>00<br>12<br>5 | 1.<br>4       | 0<br>.<br>2                | 0<br>.<br>2           |
| RF+BA<br>ML      | 0.20<br>00  | -           | -             | -             | 0.453        | 0.1072        | 0.1182        | 0.1412        | 2.72        | 0.<br>01<br>32<br>2 | 51<br>.1<br>2 | 0<br>.<br>4<br>3<br>6<br>0 | 0<br>.<br>6<br>4<br>0 |
| KRR+B<br>OB      | 0.06<br>70  | -           | -             | -             | 0.094        | 0.0950        | 0.1222        | 0.1482        | 13.22       | 0.<br>00<br>36<br>6 | 0.<br>99      | 0<br>.<br>4<br>2<br>9<br>5 | 0<br>.<br>2<br>9<br>9 |
| KRR+H<br>DAD     | 0.02<br>53  | -           | -             | -             | 0.046        | 0.0664        | 0.0844        | 0.1072        | 23.12       | 0.<br>00<br>19<br>3 | 1.<br>64      | 0<br>.<br>3<br>3<br>5      | 0<br>.<br>1<br>7<br>7 |
| GG               | 0.04<br>23  | -           | -             | -             | 0.086        | 0.0569        | 0.0630        | 0.0879        | 6.24        | 0.<br>00<br>43<br>3 | 6.<br>32      | 0<br>.<br>2<br>4<br>9      | 0<br>.<br>1<br>6<br>3 |
| enn-s2s          | 0.01<br>96  | 0.01<br>96  | 0.0170        | 0.0190        | 0.042        | 0.0428        | 0.0376        | 0.0690        | 1.92        | 0.<br>00<br>15<br>4 | 0.<br>20      | 0<br>.<br>0<br>3<br>2      | 0<br>.<br>0<br>9<br>4 |
| DTNN             | 0.03<br>66  | 0.03<br>79  | 0.0387        | 0.0359        | 0.090        | 0.0984        | 0.1056        | 0.1504        | 4.25        | 0.<br>00<br>31<br>4 | 0.<br>32      | 0<br>.<br>2<br>5<br>9      | 0<br>.<br>1<br>3<br>3 |
| SchNet           | 0.01<br>35  | 0.01<br>90  | 0.0198        | 0.0184        | 0.069        | 0.0510        | <b>0.0374</b> | 0.0797        | 3.85        | 0.<br>00<br>17<br>4 | 0.<br>30      | 0<br>.<br>0<br>7<br>3      | 0<br>.<br>0<br>7<br>5 |
| MGCN             | <b>0.01</b> | <b>0.01</b> | <b>0.0148</b> | <b>0.0164</b> | <b>0.040</b> | <b>0.0423</b> | 0.0576        | <b>0.0644</b> | <b>1.69</b> | <b>0.</b>           | <b>0.</b>     | 0                          | <b>0</b>              |

|  |    |    |  |  |  |  |  |  |  |    |    |   |   |
|--|----|----|--|--|--|--|--|--|--|----|----|---|---|
|  | 30 | 45 |  |  |  |  |  |  |  | 00 | 13 | . | . |
|  |    |    |  |  |  |  |  |  |  | 11 |    | 0 | 0 |
|  |    |    |  |  |  |  |  |  |  | 5  |    | 5 | 3 |
|  |    |    |  |  |  |  |  |  |  |    |    | 8 | 2 |

Table 1 shows that MGCN has the best show in 11 out of the 13 characteristics, with 11 of them beating substance precision. In the class, our refining model is awesome. We decide to look at the DTNN and Sch Net, two cutting-edge models, in the ANI-1 trial. As Table 2 shows, there are two reasons why the exactness values in ANI-1 are lower than in QM9. First off, the power in QM9 balance particles is negligible, but in ANI-1 off-harmony atoms, this component enhances the complexity of quantum cooperation's. Second, fitting ANI-1 is more difficult because to its significantly larger size than QM9. However, our model really achieves respectable accuracy and outperforms other methods.

**Table 2:** Accurate prediction of various models in ANI-1

| Methods | DTNN  | SchNet | MGCN  |
|---------|-------|--------|-------|
| MAE     | 0.115 | 0.110  | 0.080 |

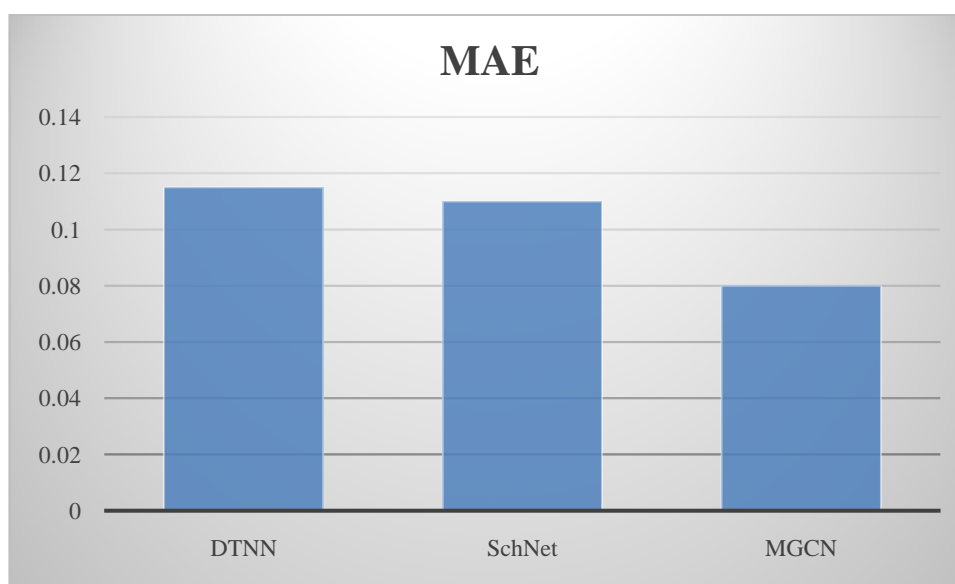


**Figure 2:** Accurate prediction of various models in ANI-1

In short, the multi-level cooperative presenting maximizes the presentation acquired by our strategy. The outcomes demonstrate that our model fits the huge dataset well and can handle both off-balance and harmony particles. For our other investigations, we utilized QM9 as our default dataset because most prior research had not included trials in the ANI-1 dataset.

**Effectiveness of multilevel interactions.** The more atoms there are in a particle, the more complex the quantum interactions get in the molecular framework. Therefore, when particle sizes increase, it becomes extremely harder to show particle cooperation.

For instance, this model's performance is often inferior to our MGCN, which has an MAE of 0.03683, when taking the expectation of U property into account. This validates the viability of our multilayer display by indicating that the molecular representations supplied by multilevel communication levels are more resilient.

**Generalizability.** In engineered space, a lot more anticipated atoms exist, however our insight into them is still very restricted. Inferable from the size constraints of the datasets that are at present open, the ideal model absolute requirement to have the option to perform successfully with negligible information. Consequently, the generalizability of these models is one more critical point from which to evaluate them.

In Table 3, the MGCN gets the least MAE of the three readiness sets. Since multi-facet coordinated efforts are shown, the molecular portrayal of MGCN is more generalizable when how much open data is more modest, in any event, when the readout times of Sch Net and MGCN are same.

**Table 3:** Comparing performance in training sets of different sizes

| N       | SchNet | DTNN   | enn-s2s | MGCN   |
|---------|--------|--------|---------|--------|
| 50,000  | 0.0258 | 0.0410 | 0.0250  | 0.0230 |
| 100,000 | 0.0149 | 0.0366 | -       | 0.0144 |
| 110,462 | 0.0136 | -      | 0.0196  | 0.0130 |

## 5. CONCLUSION

Considering all of this, it is clear that quantum chemistry can function as an essential tool for unravelling the complex world of molecular characteristics. Its ability to predict the future has altered how we study and understand the behaviours of atoms and particles, beyond traditional compound boundaries and ushering in a new era of precision and control at the molecular level. Quantum chemistry has advanced our understanding of logic and had real, substantial effects in areas like pharmaceuticals, materials science, and ecological chemistry. Its applications range from deciphering electronic designs to figuring out response components and enhancing materials. As long as we continue to restrain the power of quantum chemistry, its actual potential for development and revelation remains

enormous, with the potential to influence and upend countless aspects of our lives in the years to come.

## REFERENCES

1. Behler, J. 2014. *Representing potential energy surfaces by high-dimensional neural network potentials*. *Journal of Physics: Condensed Matter* 26(18):183001.
2. Cramer, C. J., & Truhlar, D. G. (2009). *Quantum Chemistry in Solvation and Prediction of Molecular Properties*. *Annual Review of Physical Chemistry*, 60, 93-115.
3. Johnson, B. R., & Sales, P. J. (2018). *Quantum Chemistry Approaches for Predicting Molecular Properties*. *Chemical Reviews*, 118(3), 10709-10725.
4. Korth, M., & Mayes, H. B. (2020). *Quantum Chemical Predictions of Molecular Properties for Drug Discovery*. *Journal of Medicinal Chemistry*, 63(10), 5267-5281.
5. Liu, Q.; Huang, Z.; Huang, Z.; Liu, C.; Chen, E.; Su, Y.; and Hu, G. 2018. *Finding similar exercises in online education systems*. In *Proceedings of the 24th ACM SIGKDD International Conference on Knowledge Discovery & Data Mining*, 1821–1830. ACM.
6. McDonagh, J. L.; Silva, A. F.; Vincent, M. A.; and Popelier, P. L. 2017. *Machine learning of dynamic electron correlation energies from topological atoms*. *Journal of chemical theory and computation* 14(1):216–224.
7. Schutt, K.; Kindermans, P.-J.; Felix, H. E. S.; Chmiela, S.; Tkatchenko, A.; and Muller, K.-R. 2017a. *Schnet: A continuous-filter convolutional neural network for modeling quantum interactions*. In *NIPS*, 992–1002.
8. Shao, Y., & Head-Gordon, M. (2015). *Quantum Chemistry Predictions of Spectroscopic Properties in Complex Systems*. *Chemical Society Reviews*, 44(2), 4572-4590.
9. Zhu, W.; Lan, C.; Xing, J.; Zeng, W.; Li, Y.; Shen, L.; Xie, X.; et al. 2016. *Co-occurrence feature learning for skeleton based action recognition using regularized deep lstm networks*. In *AAAI*, volume 2, 6.